DEUTSCHES ELEKTRONEN-SYNCHROTRON

DESY 94-069
April 1994

Reconstruction of the Decay $B^- \to D_1^0(2414)\pi^-$

The ARGUS Collaboration

ISSN 0418-9833

NOTKESTRASSE 85 - 22603 HAMBURG

To be sure that your preprints are promptly included in the HIGH ENERGY PHYSICS INDEX, send them to (if possible by air mail):

DESY **Bibliothek** **Notkestraße 85** **22603 Hamburg** **Germany**	**DESY-IfH** **Bibliothek** **Platanenallee 6** **15738 Zeuthen** **Germany**

DESY 94-069
April 1994

ISSN 0418-9833

Reconstruction of the Decay $B^- \to D_1^0(2414)\pi^-$

The ARGUS Collaboration

H. Albrecht, T. Hamacher, R. P. Hofmann, T. Kirchhoff, R. Mankel[1], A. Nau, S. Nowak[1], H. Schröder, H. D. Schulz, M. Walter[1], R. Wurth
DESY, Hamburg, Germany

C. Hast, H. Kapitza, H. Kolanoski, A. Kosche, A. Lange, A. Lindner, M. Schieber, T. Siegmund, B. Spaan, H. Thurn, D. Töpfer, D. Wegener
Institut für Physik[2], Universität Dortmund, Germany

P. Eckstein, K. R. Schubert, R. Schwierz, R. Waldi
Institut für Kern- und Teilchenphysik[3], Technische Universität Dresden, Germany

K. Reim, H. Wegener
Physikalisches Institut[4], Universität Erlangen-Nürnberg, Germany

R. Eckmann, H. Kuipers, O. Mai, R. Mundt, T. Oest, R. Reiner, W. Schmidt-Parzefall
II. Institut für Experimentalphysik, Universität Hamburg, Germany

J. Stiewe, S. Werner
Institut für Hochenergiephysik[5], Universität Heidelberg, Germany

K. Ehret, W. Hofmann, A. Hüpper, K. T. Knöpfle, J. Spengler
Max-Planck-Institut für Kernphysik, Heidelberg, Germany

P. Krieger[6], D. B. MacFarlane[7], J. D. Prentice[6], P. R. B. Saull[7], K. Tzamariudaki[7], R. G. Van de Water[6], T.-S. Yoon[6]
Institute of Particle Physics[8], Canada

C. Frankl, D. Reßing, M. Schmidtler, M. Schneider, S. Weseler
Institut für Experimentelle Kernphysik[9], Universität Karlsruhe, Germany

G. Kernel, P. Križan, E. Križnič, T. Podobnik, T. Živko
Institut J. Stefan and Oddelek za fiziko[10], Univerza v Ljubljani, Ljubljana, Slovenia

V. Balagura, I. Belyaev, S. Chechelnitsky, M. Danilov, A. Droutskoy, Yu. Gershtein, A. Golutvin, I. Korolko, G. Kostina, D. Litvintsev, V. Lubimov, P. Pakhlov, S. Semenov, A. Snizhko, I. Tichomirov, Yu. Zaitsev
Institute of Theoretical and Experimental Physics, Moscow, Russia

Abstract

We present the results of a partial reconstruction of the decay channel $B^- \to D_J^{(*)0}\pi^-$ performed using the ARGUS detector operating at the e^+e^- storage-ring DORIS II. In the context of this paper, $D_J^{(*)0}$ is an L=1 excited charm meson decaying to $D^{*+}\pi^-$. The measured product of branching ratios is $Br(B^- \to D_1^0(2414)\pi^-) \cdot Br(D_1^0 \to D^{*+}\pi^-)$ $= (0.17 \pm 0.05 \pm 0.04)\%$ where the first error is statistical and the second systematic. No evidence for the decay $B^- \to D_2^{*0}(2459)\pi^-$ is observed. We calculate the upper limit $Br(B^- \to D_2^{*0}(2459)\pi^-) \cdot Br(D_2^{*0} \to D^{*+}\pi^-) < 0.07\%$ at the 90% confidence level.

Recently, interest in the production of L=1 excited charm mesons in B meson decay has been widespread [1-4]. Most of this attention has been focussed on semileptonic processes for which there is a reasonably well established theoretical description [5][6]. Recent developments in heavy quark effective theory (HQET)[7] have also contributed to the theory of these decays [6,8-11]. HQET takes advantage of heavy-flavour and spin symmetries which arise as the heavy quark mass increases since the light degrees of freedom are then uncoupled from those of the heavier quark. Then rates for B decays to two states related by this symmetry are governed by the same form factor. In the case of the D, D^* this function ξ is called the Isgur-Wise function. Much of the experimental work on HQET has gone into the measurement of this function, but there also exist functions $\tau_{\frac{1}{2}^+}$ and $\tau_{\frac{3}{2}^+}$ which relate transitions to members of the two $D_J^{(*)}$ spin multiplets in the mass region of 2.4-2.5 GeV/c^2.

There are four L=1 excited charm mesons, corresponding to the coupling of one unit of orbital angular momentum with spin 0 or 1, forming a spin singlet ($^1P_1$) state and a spin triplet of states ($^3P_2, ^3P_1, ^3P_0$) with $J^P = 1^+$ and $2^+, 1^+, 0^+$ respectively. In a heavy-light meson the two 1^+ states are expected to mix to form the physical states since there is no conserved quantum number preventing them from doing so[12]. In the limit as the charm quark mass is taken to infinity this mixing is expected to result in one narrow 1^+ state degenerate in mass with the 2^+ state and one broad 1^+ state degenerate with the 0^+ state[12][13]. In the heavy quark limit the spin of the light degrees of freedom are separately conserved. It has therefore become conventional to label the heavy quark states (*ie.* in the infinite mass limit) by the spin-parity of the light degrees of freedom. Written in this notation, the four L=1 charm mesons are [8]

$$|2^+_{3/2}> \;=\; |^3P_2> \tag{1}$$

$$|1^+_{3/2}> \;=\; \sqrt{\frac{2}{3}}|^1P_1> + \sqrt{\frac{1}{3}}|^3P_1> \tag{2}$$

$$|1^+_{1/2}> \;=\; \sqrt{\frac{1}{3}}|^1P_1> - \sqrt{\frac{2}{3}}|^3P_1> \tag{3}$$

$$|0^+_{1/2}> \;=\; |^3P_0> \tag{4}$$

[1] DESY, IfH Zeuthen
[2] Supported by the German Bundesministerium für Forschung und Technologie, under contract number 054DO51P.
[3] Supported by the German Bundesministerium für Forschung und Technologie, under contract number 056DD11P.
[4] Supported by the German Bundesministerium für Forschung und Technologie, under contract number 054ER12P.
[5] Supported by the German Bundesministerium für Forschung und Technologie, under contract number 055HD21P.
[6] University of Toronto, Toronto, Ontario, Canada.
[7] McGill University, Montreal, Quebec, Canada.
[8] Supported by the Natural Sciences and Engineering Research Council, Canada.
[9] Supported by the German Bundesministerium für Forschung und Technologie, under contract number 055KA11P.
[10] Supported by the Ministry of Science and Technology of the Republic of Slovenia and the Internationales Büro KfA, Jülich.

where the subscripts label the spin-parity of the light degrees of freedom.

The experimentally observed states, the $D_1^0(2414)$[14][15] and $D_2^{*0}(2459)$[15-17], are generally associated with the states (1) and (2). Bjorken[18] has shown that the Isgur-Wise functions $\tau_{\frac{1}{2}+}$, and $\tau_{\frac{3}{2}+}$ are involved in a sum rule for the slope of ξ at zero recoil. It has been suggested[9] that nonleptonic weak decays of B mesons to $D_J^{(*)}$ mesons might provide valuable information about these functions. To date the only published studies of hadronic $B \to D_J^{(*)}$ decays, coming from ARGUS[3] and CLEO[4], have been very low statistics measurements of the channels $B^- \to D_J^{(*)0}\pi^{-\dagger}$ and $B^- \to D_J^{(*)0}\rho^-$. Such two body decays, of course, do not provide a great deal of information about the Isgur-Wise functions since they contain information at only one value of q^2. However, one does need these functions evaluated at the proper value of q^2 in order to predict branching fractions. Such predictions have been made by two groups[9][11], and the results differ sufficiently that the measurement of $Br(B^- \to D_1^0(2414)\pi^-)$ does discriminate between the two models. Owing to the low statistics available and the fact that the two observable states, $D_1^0(2414)$ and $D_2^{*0}(2459)$, with natural widths of about 20 MeV/c^2, combine to form a large $D_J^{(*)0}$ mass region, previous measurements were unable to distinguish contributions from individual $D_J^{(*)0}$ states. This paper presents the results of an analysis of the decay sequence

$$\begin{array}{rcl} B^- & \to & D_J^{(*)0}\pi_1^- \\ & & \hookrightarrow D^{*+}\pi_2^- \\ & & \hookrightarrow D^0\pi_3^+ \end{array} \qquad (5)$$

which does not require reconstruction of the D^0 meson. This leads to a significant increase in statistics since the D^0 final states which are usually reconstructed represent only about 15-20% of the D^0 decay width. The previous ARGUS analysis[3] of this channel had an efficiency×branching ratio (ϵ·Br) of about 2%. Use of the partial reconstruction technique, described below, results in an ϵ·Br of about 11%. Partial reconstructions have been used by both ARGUS and CLEO in the analysis of the decay $\bar{B}^0 \to D^{*+}\pi^-$[19][20] and by ARGUS in the analysis of the semileptonic decays $\bar{B}^0 \to D^{*+}\ell^-\bar{\nu}_\ell$[21] and $B^- \to \rho^0\ell^-\bar{\nu}_\ell$[22].

The analysis presented here is based on data collected at center-of-mass energies around 10 GeV using the ARGUS detector at the DORIS II e^+e^- storage ring at DESY. The data sample used comprises an integrated luminosity of 246 pb^{-1} taken on the $\Upsilon(4S)$ resonance and 97 pb^{-1} in the nearby continuum. The $\Upsilon(4S)$ data corresponds to 208000 ± 9800 $B\bar{B}$ pairs assuming the $\Upsilon(4S)$ decays only to B mesons. We assume here that pairs of charged and neutral B mesons are produced in equal proportion. The ARGUS detector is a large solid angle spectrometer described in detail elsewhere[23]. The charged tracks used in this analysis were required to come from the main vertex and to have $p_T > 0.06$ GeV/c and $|\cos\theta| < 0.92$, where p_T is the transverse momentum and θ is the angle between the track momentum and the beamline. Charged particle identification is made on the basis of specific

†References in this paper to a specific charge state also imply the charge conjugate state.

ionization and time-of-flight measurements. For lepton identification information from the shower counters and muon chambers was also included. All this information was combined to form a likelihood ratio for each of the particle hypotheses, e, μ, π, K, and p. All particle hypotheses with a likelihood in excess of 1% were accepted. Photons were identified as energy deposits in the electromagnetic calorimeter not associated with any charged track.

The particles π_1, π_2 and π_3 produced in the sequential two-body decay chain (5) contain sufficient kinematical information to allow determination of the $D_J^{(*)0}$ mass without reconstruction of the D^0. The information may be obtained from the quantities $\vec{P}_{\pi_1}$,$\vec{P}_{\pi_2}$, $\vec{P}_{\pi_3}$, M_π, M_D, M_{D^*} M_B, and $|\vec{P}_B|$ where

$$|\vec{P}_B| = \sqrt{E_{beam}^2 - M_B^2}. \qquad (6)$$

With $\vec{P}_1 = \vec{P}_{\pi_1}$, $\vec{P}_{12} = \sum_{i=1}^{2}\vec{P}_{\pi_i}$, $\vec{P}_{123} = \sum_{i=1}^{3}\vec{P}_{\pi_i}$, $E_1 = E_{\pi_1}$, $E_{12} = \sum_{i=1}^{2}E_{\pi_i}$, and $E_{123} = \sum_{i=1}^{3}E_{\pi_i}$ the vector and scalar equalities

$$\vec{P}_B = \vec{P}_{D_J^{(*)}} + \vec{P}_1 \qquad E_B = E_{D_J^{(*)}} + E_1 \qquad (7)$$

$$\vec{P}_B = \vec{P}_{D^*} + \vec{P}_{12} \qquad E_B = E_{D^*} + E_{12} \qquad (8)$$

$$\vec{P}_B = \vec{P}_D + \vec{P}_{123} \qquad E_B = E_D + E_{123} \qquad (9)$$

allow one to solve for the scalar products

$$\mathbf{X}_1 \equiv \vec{P}_B \cdot \vec{P}_{12} = -\frac{1}{2}\left(M_B^2 + M_{12}^2 - 2E_B E_{12} - M_{D^*}^2\right) \qquad (10)$$

$$\mathbf{X}_2 \equiv \vec{P}_B \cdot \vec{P}_{123} = -\frac{1}{2}\left(M_B^2 + M_{123}^2 - 2E_B E_{123} - M_D^2\right). \qquad (11)$$

Using the decomposition

$$\vec{P}_B = A\vec{P}_{12} + B\vec{P}_{123} + C\vec{P}_x \qquad (12)$$

$$\vec{P}_x = \frac{\vec{P}_{12} \times \vec{P}_{123}}{|\vec{P}_{12}||\vec{P}_{123}|} \qquad (13)$$

which is valid so long as $\vec{P}_{12}$ and $\vec{P}_{123}$ are not parallel, we can write

$$\vec{P}_B \cdot \vec{P}_{12} = AP_{12}^2 + B\vec{P}_{12} \cdot \vec{P}_{123} = \mathbf{X}_1 \qquad (14)$$

$$\vec{P}_B \cdot \vec{P}_{123} = BP_{123}^2 + A\vec{P}_{12} \cdot \vec{P}_{123} = \mathbf{X}_2 \qquad (15)$$

which leaves two equations in the two unknown coefficients A and B. Solving these equations we obtain

$$A = \frac{(\mathbf{X}_1)P_{123}^2 - (\mathbf{X}_2)(\vec{P}_{123} \cdot \vec{P}_{12})}{P_{123}^2 P_{12}^2 - (\vec{P}_{123} \cdot \vec{P}_{12})^2} \qquad (16)$$

$$B = \frac{(\mathbf{X}_2)P_{12}^2 - (\mathbf{X}_1)(\vec{P}_{123} \cdot \vec{P}_{12})}{P_{123}^2 P_{12}^2 - (\vec{P}_{123} \cdot \vec{P}_{12})^2}. \qquad (17)$$

Squaring equation (12) and using (16) and (17) we can solve for C to within a sign ambiguity;

$$C = \pm\sqrt{\frac{P_B^2 - (AP_{12})^2 - (BP_{123})^2 - 2AB(\vec{P}_{123}\cdot\vec{P}_{12})}{P_x^2}}. \tag{18}$$

A solution for $\vec{P}_B$ allows for the calculation of the $D_J^{(*)}$ mass using (7). The two solutions for C yield two solutions ($\tilde{M}_\pm$) for the pseudomass. Fitting the $\tilde{M}_+$ and $\tilde{M}_-$ distributions separately and averaging produces results similar to those obtained by averaging the two solutions before plotting. The latter procedure, however, produces slightly better resolution. We define the pseudomass $\tilde{M}$ and pseudomass-difference $\delta\tilde{M}$ by

$$\tilde{M} = \frac{1}{2}(\tilde{M}_+ + \tilde{M}_-), \quad \delta\tilde{M} = |\tilde{M}_+ - \tilde{M}_-|. \tag{19}$$

Figure 1 shows the results of a Monte Carlo analysis of 10,000 events containing the decay sequence (5). All events were subjected to a full detector simulation[23]. Figure 1(a) shows the momentum regions populated by the three pions from the sequential decay (5). The three regions are almost distinct so in the analysis of real data one can differentiate between the three pions by using momentum cuts. There is overlap only between the momentum spectra of π_2^- and π_3^+ which are oppositely charged and hence cannot be exchanged to produce another entry with the same π_1^-. In performing the actual analysis the allowed momentum regions are broadened since restricting to the kinematically allowed regions shown in Figure 1(a) would result in the population of only a limited region of the mass plot, making background analysis difficult. In this analysis we define the momentum regions (units of GeV/c)

$$(1.0 < P_{\pi_1} < 2.3),\ (0.06 < P_{\pi_2} < 1.0),\ (0.06 < P_{\pi_3} < 0.23), \tag{20}$$

where the lower bounds on P_{π_2} and P_{π_3} are due to requirements on p_T. The pseudomass spectrum obtained from the Monte Carlo data sample is shown in Figure 1(b). Here we have added the requirement that $\delta\tilde{M}$ be less than 60 MeV/c^2. This is about 80% efficient and eliminates a small systematic mass shift which occurs if high $\delta\tilde{M}$ entries are retained. It also results in a small (10%) improvement in resolution. Overlaid on the histogram is the result of a fit with a third-order polynomial background function times a threshold factor and a Gaussian to parametrize the signal. D_1^0 mesons were generated at a mass of 2414 MeV/c^2 with a natural width of 15 MeV/c^2. The fitted mass is 2413.9 $\pm$ 0.7 MeV/c^2 in good agreement with the generated value. The resolution is 22$\pm$1 MeV/c^2. The efficiency, without further cuts, is about 25%. Overlaid as a shaded histogram is the pseudomass distribution obtained from the wrong sign combinations $\pi_1^-\pi_2^+\pi_3^+$ (the sign of π_2 has been flipped). This distribution has been scaled down to account for a slightly different normalization which arises due to overlap of the π_2 and π_3 momentum regions. Using Monte Carlo, this scale factor has been shown to be 0.86 $\pm$ 0.04 for both correlated and random $\pi_1^-\pi_2^+\pi_3^+$ combinations. Figure 1(b) shows that the correlated background underneath the

Monte Carlo signal is due primarily to random π_2's. In the experimental data there will be further contributions to this background when a random π_2^- is combined with a real (π_1^-, π_3^+) pair from the decay sequence

$$\begin{aligned} \bar{B}^0 \;&\rightarrow\; D_J^{(*)+}\pi_1^- \\ &\quad\hookrightarrow D^{*+}\pi^0 \\ &\qquad\hookrightarrow D^0\pi_3^+. \end{aligned} \tag{21}$$

Monte Carlo studies of other decay sequences which might be expected to produce correlated background, such as $B^- \rightarrow D_J^{(*)0}\rho^-$ and $\bar{B}^0 \rightarrow D^{*+}\pi^-$, show them to produce negligible signal contributions and contributions to the background distribution which are well described by the wrong-sign combinations $\pi_1^-\pi_2^+\pi_3^+$.

In the analysis of the experimental data there will be background contributions coming from continuum $q\bar{q}$ events (primarily $c\bar{c}$). To suppress these contributions we apply the following additional selection criteria; we require that an event have $H_2 < 0.3$, where H_2 is the second Fox-Wolfram moment[24], thus suppressing acceptance of high thrust continuum events. We further require that the event be kinematically consistent with being a B meson decay in that it contain no track with momentum greater than 2.3 GeV/c and that the total multiplicity $n_{ch} + \frac{1}{2}n_\gamma$ of the event be greater than 5 where n_{ch} is the number of charged tracks and n_γ is the number of photons with energy greater than 50 MeV. To ensure that the fast track (π_1) is well measured, we require $|\cos\theta| < 0.85$. The allowed momentum regions for the three pion tracks were given in (20). Pions consistent with coming from K_S^0 decays were removed from the analysis as were tracks consistent with being electrons from photon conversion. This was done by excluding from the analysis $\pi^+\pi^-(e^+e^-)$ track pairs fitting to a secondary vertex, having an invariant mass within $\pm$30 MeV/c^2 of the nominal K_S^0 (γ) mass and a χ^2 of less than 16 for the appropriate mass hypothesis. In the π_1 momentum region lepton identification is very good. In order to eliminate contributions from semileptonic decays, which are kinematically very similar in the soft neutrino limit, all tracks having a lepton likelihood of greater than 70% were excluded from further analysis (for muons we also required hits in the outer muon chambers). That this successfully eliminates contributions due to semileptonic decays was demonstrated in Monte Carlo studies as well as in the analysis of semileptonic events selected from the data. As suggested by the Monte Carlo studies discussed earlier, we required $\delta\tilde{M} < 60$MeV/c^2. After all these cuts, a great deal of the background from continuum events remains. Monte Carlo studies show that the continuum events which contribute are primarily $c\bar{c}$ events in which fragmentation of the charm quarks produces at least one D^{*+}. In these events the slow π_3 usually comes from the D^{*+} while the π_1 candidate comes from the final products of a D meson decay, which are a mixture of pions and kaons. In light of this we make one final cut against the continuum by requiring that the kaon likelihood of the π_1 candidate be less than 15%. The efficiency for this cut on real pions in the kinematically allowed momentum region was calculated from

the data using the decay pions from K^0_S decays reconstructed at secondary vertices. For the remainder of the selection criteria the efficiency is obtained using Monte Carlo. The overall efficiency for the cuts described above is just under 17%.

The use of a partial reconstruction technique implies a certain loss of information; this is the price paid for the increase in statistics. In this analysis the information lost is that concerning the decay angle of the $D_J^{(*)0}$, defined as the angle between the pion from the $D_J^{(*)0}$ decay and $D_J^{(*)0}$ flight direction in the $D_J^{(*)0}$ rest frame, and the angle between the pion from the $D_J^{(*)}$ decay and the pion from the D^* decay in the D^{*+} rest frame. Distributions in these angles depend, respectively, on the $D_J^{(*)0}$ polarization[25] and spin-parity[12]. The resolution of the partial reconstruction technique described above is good only for scalar quantities such as mass or $|p|$; individual components of momenta are only poorly resolved. Thus one cannot accurately calculate the Lorentz boost vectors to the rest frames in which these angular distributions are defined. Since one cannot measure these distributions it is important to show that the efficiency is independent of them. This has been done using Monte Carlo. A similar argument applies to the B meson production angle. B mesons produced on the $\Upsilon(4S)$ resonance have a $\sin^2\theta_B$ distribution with respect to the beamline. Selection criteria based on this angle are useful in full reconstructions. However, in the analysis presented in this paper, this information is unavailable. Monte Carlo simulation shows that the reconstruction efficiency in this analysis is independent of the B meson production angle.

The pseudomass distribution obtained using the cuts described above is shown in Figure 2(a) as solid points with error bars. Overlaid as a shaded histogram is the pseudomass distribution obtained by selecting the wrong-sign combinations $\pi_1^-\pi_2^+\pi_3^+$. Since this wrong-sign distribution contains the correlated background from (5) and (21), and should contain the same random background, this distribution is expected to provide a good description of the background. The wrong-sign distribution has been scaled down to adjust for the normalization difference discussed earlier. The scale factor is consistent with the one obtained from Monte Carlo. Overlaid as a solid line is the result of a fit using a third-order polynomial background times a threshold factor to describe the background and a Gaussian to describe the signal. The width of the Gaussian has been fixed to the Monte Carlo value of 22 MeV/c^2. This fit yields 40±11 events at a mass of 2412±7 MeV/c^2. The mass is consistent with the previous ARGUS mass determination[14] so we continue to refer to this state as the $D_1^0(2414)$. There are no events producing multiple entries in the signal region. Figure 2(b) shows the wrong-sign distribution fitted with the same function with the mass of the Gaussian fixed to the value determined above. The fit yields 1±8 events. Overlaid as a dotted line is the fit result from Figure 2(a). The background fits to the right and wrong sign distributions agree excellently. It is also apparent in Figure 2(a) that the wrong-sign distribution provides a good description of the background as anticipated.

This analysis has also been performed on the continuum data to ensure that there is

Theory	$B^- \to (D^{*+}\pi^-)_{res}\pi^-$	$1^+_{3/2}$	$2^+_{3/2}$	$1^+_{1/2}$
Reader, Isgur [9]	0.15%	0.10%	0.025%	0.025%
Colangelo et al [11]	0.08%	0.027%	0.012%	0.040%

Table 1: Theoretical predictions for the resonant part of the $B^- \to D^{*+}\pi^-\pi^-$ branching ratio and rates through individual intermediate resonant states.

no signal contribution from continuum events. In this analysis all momenta were scaled up[‡] to account for the different values of $\sqrt{s}$. No enhancement in the signal region was observed. Continuum contributions to the signal were also searched for using data taken on the $\Upsilon(4S)$ resonance by examining the pseudomass distribution obtained from events having a high second Fox-Wolfram moment. Again, no evidence for such contributions was observed. This analysis also showed that continuum distributions are well described by the wrong-sign combinations; the fit to the wrong sign distribution is therefore further evidence that continuum contributions to the signal are small.

From the results of the fit to the pseudomass distribution in Figure 2(a), and using $Br(D^{*+} \to D^0\pi^+) = (68.1 \pm 1.0 \pm 1.3)\%$[26], we calculate the product of branching ratios

$$Br(B^- \to D_1^0\pi^-)\, Br(D_1^0 \to D^{*+}\pi^-) = (0.17 \pm 0.05 \pm 0.04)\% \qquad (22)$$

where the first error is statistical and the second systematic. Contributions to the systematic error come from variation of the fit parameters (including variation of the Gaussian width to account for the large error on the measured value of the D_1^0 natural width[14]), the efficiency calculation, the number of $B\bar{B}$ pairs and the error on the D^{*+} branching ratio. This result agrees well with the previous experimental results which did not discriminate between the 1^+ and 2^+ states.

Recent theoretical treatments using HQET and factorization have provided predictions for the $D_J^{(*)0}$ resonant contribution to the $B^- \to D^{*+}\pi^-\pi^-$ rate. The results of Reader and Isgur[9], and those of Colangelo et al.[11] are summarized in Table 1. The two models differ primarily in their treatments of the function $\tau_{\frac{3}{2}+}$. Reader and Isgur use a sum rule to relate $\tau_{\frac{3}{2}+}$ to ρ^2, the slope of ξ at zero recoil. For ρ^2 they use the value obtained experimentally from fits to $\bar{B}^0 \to D^{*+}l^-\bar{\nu}_l$ data (1.18 ± 0.50)[27]. Close and Wambach[28] have shown that this value is consistent with theoretical predictions. Colangelo et al. calculate the Isgur-Wise functions $\tau_{\frac{1}{2}+}$ and $\tau_{\frac{3}{2}+}$ using QCD sum rules[10]. Their prediction is substantially lower than the observed rate. That of Reader and Isgur is consistent with the observed value although still somewhat lower. No errors are quoted by the either group but both provide some arguments as to why the errors might be small. Both groups obtain sizable contributions from the intermediate $2^+_{3/2}$ state relative to that through $1^+_{3/2}$. Such rates to the $D_2^{*0}(2459)$ might be expected to make that state observable in this analysis. In the calculation of Reader and Isgur, which yields the best agreement with the observed rate

[‡]Alternatively one can scale down the value of M_B. These procedures yield consistent results.

through the $D_1^0(2414)$ intermediate state, predictions for the (relative) rates would lead to signals of about 10 events in each of the two other states. The undiscovered $1^+_{1/2}$ state is expected to be broad[29], making a signal of this size unobservable, but 10 events at the $D_2^{*0}(2459)$ mass might be observable as a shoulder on the signal from the lower mass 1^+ state or at least as a broadening of the signal width. The D_2^{*0} mass is indicated in Figure 2(a) - no such effect is observed. In fact, fitting the pseudomass distribution with a free width results in a narrower rather than a larger than expected width.[§] Assuming a natural width of 19 MeV/c^2[30] for the 2^+ state, Monte Carlo yields a Gaussian width of 24 MeV/c^2 for the corresponding pseudomass peak. Fitting the distribution with the function used previously but with an additional Gaussian with mass and width fixed to 2459 MeV/c^2 and 24 MeV/c^2 respectively yields 41±11 events in the 1^+ signal, consistent with the number previously obtained, and −5±11 events at the 2^+ mass. This leads to the upper limit

$$Br(B^- \to D_2^{*0}(2459)\pi^-)\cdot Br(D_2^{*0} \to D^{*+}\pi^-) < 0.07\% \quad @90\%\ \text{C.L.} \tag{23}$$

In summary, using the ARGUS detector, we have measured the product of branching ratios $Br(B^- \to D_J^{(*)0}\pi^-)\cdot Br(D_J^{(*)0} \to D^{*+}\pi^-)$ with statistics sufficient to allow conclusions to be drawn about contributions from individual (narrow) states. We obtain the results

$$Br(B^- \to D_1^0(2414)\pi^-)\cdot Br(D_1^0 \to D^{*+}\pi^-) = (0.17 \pm 0.05 \pm 0.04)\% \tag{24}$$

$$Br(B^- \to D_2^{*0}(2459)\pi^-)\cdot Br(D_2^{*0} \to D^{*+}\pi^-) < 0.07\% \quad @90\%\ \text{C.L.} \tag{25}$$

It is a pleasure to thank U.Djuanda, E.Konrad, E.Michel, and W.Reinsch for their competent technical help in running the experiment and processing the data. We thank Dr.H.Nesemann, B.Sarau, and the DORIS group for the excellent operation of the storage ring. The visiting groups wish to thank the DESY directorate for the support and kind hospitality extended to them.

[§] Leaving the Gaussian width free in the fit to the pseudomass distribution results in a fit width of 18±7 MeV/c^2, consistent with the expected value of 22 MeV/c^2.

References

[1] ARGUS Collab., H.Albrecht et al., *Z. Phys.***C57** (1993) 533.

[2] CLEO Collab., S.Henderson et al., *Phys. Rev.* **D45** (1992) 2212.

[3] ARGUS Collab., H.Albrecht et al., *Z. Phys.* **C48** (1990) 543.

[4] CLEO Collab., D.Bortoletto et al., *Phys. Rev.* **D45** (1992) 21.

[5] N.Isgur et al., *Phys. Rev.* **D39** (1989) 799.

[6] D.Scora, *Semileptonic Hadron Decay in the Quark Potential Model*, Ph.D. Thesis, Universtity of Toronto, (1992). Unpublished.

[7] N.Isgur and M.Wise, *Phys. Lett.* **B232** (1989) 113, **B237** (1990) 527.

[8] N.Isgur and M.Wise, *Phys. Rev.* **D43** (1991) 819.

[9] C.Reader and N.Isgur, *Phys. Rev.* **D47** (1993) 1007.

[10] P.Colangelo et al., *Phys. Lett.* **B293** (1992) 207.

[11] P.Colangelo et al., BARI-TH/92-131 (1992).

[12] J.L.Rosner, *Comm. Nucl. Part. Phys.* **16** (1987) 321.

[13] S.Godfrey and R.Kokoski, *Phys. Rev.* **D43** (1991) 1679.

[14] ARGUS Collab., H.Albrecht et al., *Phys. Lett.* **B232** (1989) 398.

[15] CLEO Collab., P.Avery et al., *Phys. Rev.* **D41** (1990) 774.

[16] ARGUS Collab., H.Albrecht et al., *Phys. Lett.* **B221** (1989) 422.

[17] E691 Collab., J.C.Anjos et al., *Phys. Rev. Lett.* **62** (1989) 1717.

[18] J.D.Bjorken, invited talk at Les Rencontre de Physique, La Thuile, Italy, [SLAC report SLAC-PUB-5278] (1990).

[19] ARGUS Collab., H.Albrecht et al., *Phys. Lett.* **B182** (1986) 95.

[20] CLEO Collab., R.Giles et al., *Phys. Rev.* **D30** (1984) 2279.

[21] ARGUS Collab., H.Albrecht et al., DESY 93-149 (1993).

[22] *Study of the Decay $B^+ \to \rho^0 l^+ \nu$*, in *Proceedings of the 4^{th} International Symposium on Heavy Flavour Physics*, Ed. M.Davier and G.Wormser, Editions Frontières, Gis-sur-Yvette Cedex, France (1992) 249.

[23] ARGUS Collab., H.Albrecht et al., *Nucl. Instrum. Methods* **A275** (1989) 1.

[24] G.C.Fox and S.Wolfram, *Nucl. Phys.* **B149** (1979) 413.

[25] M.Lu et al., Cal.Tech. Preprint CALT-68-1741 (CEBAF-TH-91-16), (1992).

[26] CLEO Collab., F.Butler et al., *Phys. Rev. Lett.* **69** (1992) 2014.

[27] S.Stone, *Semileptonic B Decays - Experimental*, in *B Decays*, edited by S.Stone, World Scientific, Singapore (1992).

[28] F.Close and A.Wambach, RAL-93-022 (1993).

[29] S.Godfrey and N.Isgur, *Phys. Rev.* **D32** (1985) 189.

[30] Particle Data Group, M. Aguilar-Benitez et al., *Review of Particle Properties*, *Phys. Rev.* **D45** (1992) 1.

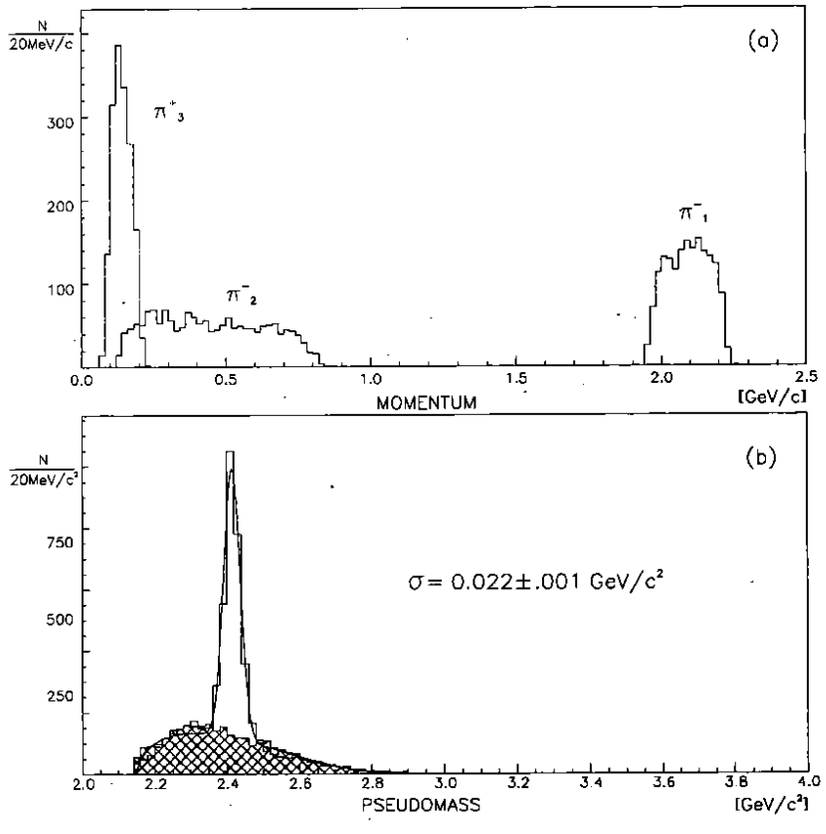

Figure 1: The results of the pseudomass analysis performed on 10,000 events containing the decay sequence (5). (a) shows the lab-frame momentum regions populated by the decay pions from (5). (b) shows the calculated pseudomass distribution. Overlaid as a solid line is the result of the fit described in the text. The hatched histogram is the scaled (see text) pseudomass distribution obtained by selecting the wrong-sign combinations $\pi_1^-\pi_2^+\pi_3^+$.

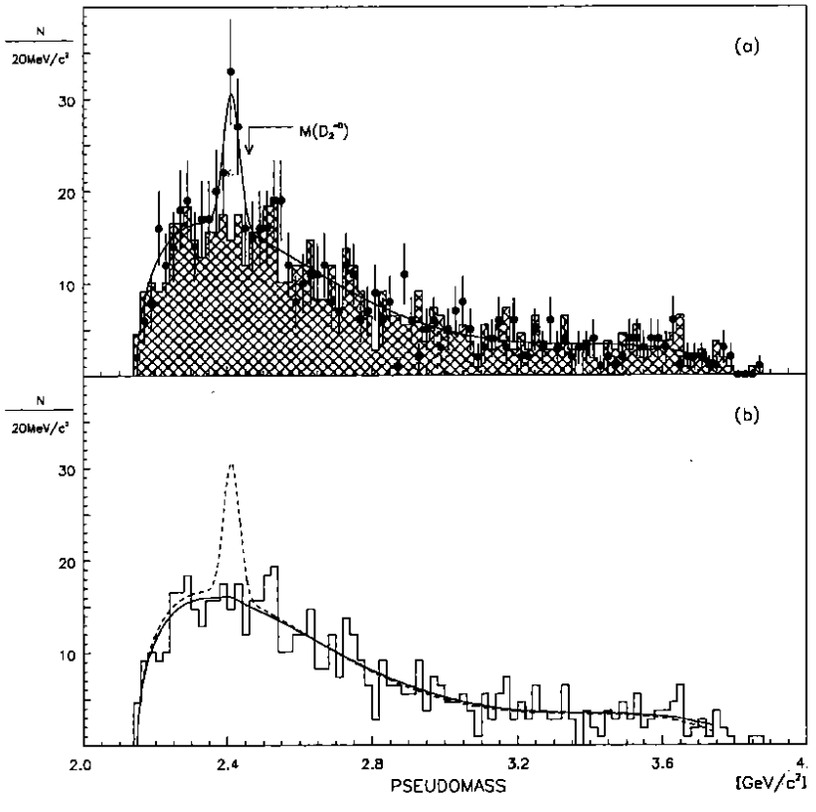

Figure 2: Pseudomass distributions from data analysis. Data selection criteria are described in the text. The distribution obtained from the right-sign combinations is shown as solid points with error bars in (a). Overlaid are the scaled wrong-sign pseudomass distribution (hatched histogram) and the result of the fit described in the text. (b) shows the wrong-sign distribution alone. Overlaid are the results of a fit to the wrong-sign distribution (solid line) as well as the fit to the right-sign distribution from (a) (dashed line). The fits are described in the text.